Eur. Phys. J. C (2023) 83:1166
https://doi.org/10.1140/epjc/s10052-023-12322-z

THE EUROPEAN PHYSICAL JOURNAL C

Regular Article - Theoretical Physics

Effect of acceleration on information delocalization

Xi Ming[1,2,a]

[1] Innovation Academy for Precision Measurement Science and Technology, Chinese Academy of Sciences, Wuhan 430071, China
[2] *Present address:* University of Chinese Academy of Sciences, Beijing 100049, China

Received: 18 July 2023 / Accepted: 4 December 2023 / Published online: 21 December 2023

Abstract We study the impact of acceleration on information delocalization under the Unruh (anti-Unruh) effect for two types of tripartite entangled states, namely the GHZ and W states. Our findings indicate that the anti-Unruh effect can result in stronger delocalization of quantum information, as measured by tripartite mutual information (TMI). Additionally, we show that the W state is more stable than the GHZ state under the influence of uniformly accelerated motion. Lastly, we extend our analysis to N-partite entangled states and product states.

1 Introduction

The delocalization of quantum information describes the dispersion of information from local degrees of freedom into the many-body degrees of freedom within a system, which is closely related to thermalization in quantum many-body dynamics [1–3]. Besides many-body systems [4,5], this captivating subject has also been extensively studied in quantum information physics [6,7] and black hole physics [8,9]. An effective measure of information delocalization is tripartite mutual information (TMI), which becomes negative when local quantum information is distributed globally [10,11]. Furthermore, smaller TMI values signify stronger information delocalization.

Another intriguing phenomenon intimately connected to black hole research is the Unruh effect [12]. Inspired by the Hawking radiation resulting from black hole evaporation [13,14], Unruh postulated that a uniformly accelerated observer in the vacuum field would detect a thermal bath with temperature $T = a/2\pi$, now known as the Unruh effect. It is evident that the temperature T of this thermal bath is proportional to the acceleration a, paralleling the temperature of Hawking radiation [13,14]. In addition to Hawking radiation, the Unruh effect contributes significantly to understanding other theories, such as cosmological horizons [15] and the thermodynamic interpretation of gravity [16,17]. The Unruh–DeWitt model, which comprises a two-level point monopole coupled with a massive or massless scalar field along its trajectory [18], is the most prominent proposal for investigating field-detector interactions. Under the Unruh effect, the transition probability of the detector increases with acceleration. Interestingly, recent research has found that the transition probability of the Unruh–DeWitt detector decreases as its acceleration increases under certain conditions. This new phenomenon is distinct from the traditional Unruh effect and is called the anti-Unruh effect [19,20].

Previous research has explored the influence of both the Unruh effect and anti-Unruh effect on various quantum resources [21–34]. In this paper, we focus on the impact of acceleration on TMI, which can characterize whether quantum information is delocalized. We adopt the Unruh–DeWitt model and assume that three observers, Alice, Bob, and Charlie, each possess identical detectors interacting with their respective massless scalar fields. Here, we consider three detectors with different initial entangled states, including GHZ and W states. We examine the evolution of TMI with acceleration when one, two, or all three observers move at the same acceleration, as shown in Fig. 1. Computational results reveal that the anti-Unruh effect can induce stronger delocalization of information than the Unruh effect across the entire system. Besides, we observe weaker delocalization of information in the W state, indicating that it is more robust than the GHZ state when subjected to uniformly accelerated motion. We also calculate the TMI for detectors initially in N-partite GHZ and product states.

This paper is organized as follows. In Sect. 2, we introduce the TMI for quantifying information delocalization and briefly review the Unruh–DeWitt model. In Sect. 3, we investigate the evolution of information delocalization for several different situations. In Sect. 4, we extend the discussion to

[a] e-mail: mingxi@wipm.ac.cn (corresponding author)

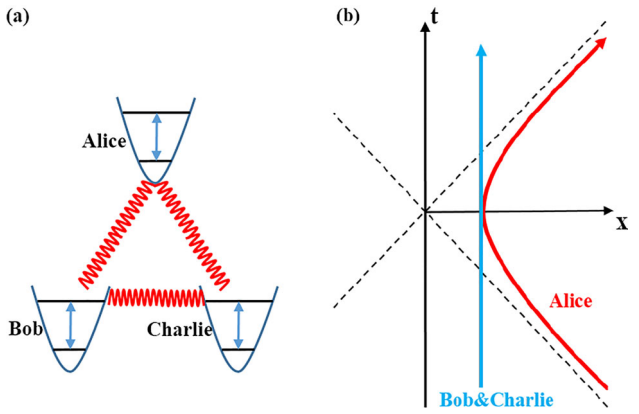

Fig. 1 **a** Alice, Bob, and Charlie individually possess identical Unruh–DeWitt detectors, and they are initially prepared in a tripartite entangled state; **b** depiction of the Minkowski spacetime shows that Alice (red hyperbola) undergoes uniform acceleration, while Bob and Charlie (blue line) remain stationary

the case of multiple detectors. Finally, we conclude our work in Sect. 5.

2 Methods

2.1 Tripartite mutual information (TMI)

For a tripartite system that contains three subsystems A, B, and C, we can introduce the von Neumann entanglement entropy, which is defined as

$$S_A = -\operatorname{tr} \rho_A \ln \rho_A, \tag{1}$$

where the reduced density matrix is $\rho_A = \operatorname{tr}_{BC} \rho_{ABC}$, and similar calculations are for the ρ_B, ρ_C, ρ_{AB}, ρ_{AC}, and ρ_{BC}. Then, we can calculate the TMI by the following form [10,11],

$$\begin{aligned} I_3 &= I(A,B) + I(A,C) - I(A,BC) \\ &= S(\rho_A) + S(\rho_B) + S(\rho_C) + S(\rho_{ABC}) \\ &\quad - S(\rho_{AB}) - S(\rho_{AC}) - S(\rho_{BC}), \end{aligned} \tag{2}$$

where the bipartite mutual information $I(A,B) = S(\rho_A) + S(\rho_B) - S(\rho_{AB})$ measures the total amount of correlations between subsystems A and B, and analogous definitions for $I(A,C)$, $I(B,C)$, and $I(A,BC)$. Due to the subadditivity of von Neumann entanglement entropy, the bipartite mutual information must be non-negative. However, the TMI can be negative when the information of subsystem A stored in composite BC is larger than the total amount of information of subsystem A stored in subsystem B and subsystem C individually, i.e., $I(A,BC) > I(A,B) + I(A,C)$ [2]. This indicates that delocalization occurs and local information spreads from the subsystem throughout the entire system. On the other hand, the positive TMI implies that more quantum information is stored among individual subsystems. Furthermore, $I_3 = 0$ if the tripartite system is a pure state or if subsystems A, B, and C are not related to each other, meaning the entire system is in a separable state. In this paper, we will utilize the TMI to quantify information delocalization.

2.2 The Unruh–DeWitt model

Next, we provide a brief overview of the Unruh–DeWitt model in this section. Consider a $(1+1)$-dimensional single-mode massless scalar field ϕ interacting with a two-level quantum system, with ground state $|g\rangle$ and excited state $|e\rangle$ separated by an energy gap Ω. The interaction Hamiltonian for this model is [18]

$$H_I = \lambda \chi(\tau/\sigma)\mu(\tau)\phi[x(\tau), t(\tau)], \tag{3}$$

where λ denotes the coupling constant, τ represents the detector's proper time along its trajectory $x(\tau)$ and $t(\tau)$, $\chi(\tau/\sigma)$ is the switching function controlling the interaction time via parameter σ, and $\mu(\tau)$ is the detector's monopole moment. We assume weak coupling with $\lambda = 0.1$, Gaussian switching function $\chi(\tau/\sigma) = \mathrm{e}^{-\tau^2/2\sigma^2}$, and $t(\tau) = a^{-1}\sinh(a\tau)$ and $x(\tau) = a^{-1}[\cosh(a\tau) - 1]$. For weak coupling, the time evolution operation can be perturbatively expanded as

$$\begin{aligned} U &= I - i\int d\tau H_I(\tau) + \mathcal{O}\left(\lambda^2\right) \\ &= -i\lambda \sum_m \left(I_{+,m} a_m^\dagger \sigma^+ + I_{-,m} a_m^\dagger \sigma^- + \text{H.c.}\right) + \mathcal{O}\left(\lambda^2\right), \end{aligned} \tag{4}$$

where we treat the spacetime as a cylinder with spatial circumference $L = 200$, m indicates the discrete mode of the scalar field with periodic boundary conditions ($k = 2\pi m/L$), $a_m(a_m^\dagger)$ represents the annihilation (creation) operator in mode m of the scalar field and satisfies $a_m|0\rangle = 0$ ($a_m^\dagger|0\rangle = |1\rangle_m$), $\sigma^\pm$ are SU(2) ladder operators, and $I_{\pm,m}$ is given by

$$I_{\pm,m} = \int_{-\infty}^{\infty} \frac{1}{\sqrt{4\pi|m|}} \chi(\tau/\sigma) \mathrm{e}^{\pm i\Omega\tau + \frac{2\pi \mathrm{i}}{L}[|m|t(\tau) - mx(\tau)]} d\tau. \tag{5}$$

Within the first-order approximation, this evolution follows that [19,31,34]

$$\begin{aligned} U|g\rangle|0\rangle &= C_+(|g\rangle|0\rangle - i\eta_+|e\rangle|1\rangle_{g,m}), \\ U|e\rangle|0\rangle &= C_-(|e\rangle|0\rangle + i\eta_-|g\rangle|1\rangle_{e,m}), \end{aligned} \tag{6}$$

where $C_\pm = 1/\sqrt{1+\eta_\pm^2}$ are normalization factors, and $\eta_\pm = \lambda \sum_{m\neq 0} I_{\pm,m}$ are connected with the excitation and deexcitation probability of the detector. It is necessary to note that the $|1\rangle_{g,m}$ and $|1\rangle_{e,m}$ are distinct in general. Nevertheless, a significant advancement is that Bruschi and his coauthors

have addressed the validity of the single-mode approximation, i.e., $|1\rangle_{g,m} = |1\rangle_{e,m}$ [23]. As a result, we adopt the single-mode approximation in this paper [35,36]. In summary, we consider the massless scalar field case and remove the zero mode in a periodic cavity. It is worth mentioning that the validity of the above conditions has been demonstrated in [20].

Consider the detector is in the ground state $|g\rangle$, the transition probability at leading order in the perturbative expansion is given by

$$P = \sum_{m\neq 0} |\langle 1|_m \langle e|U|g\rangle|0\rangle|^2 = \lambda^2 \sum_{m\neq 0} |I_{+,m}|^2. \tag{7}$$

In previous studies, the transition probability was used to discriminate between Unruh effect and anti-Unruh effect [19, 20]. Under the Unruh effect, the larger acceleration generally represents larger transition probability. Contrarily, the transition probability of the detector can decrease with acceleration in specific circumstances, which is known as the anti-Unruh effect. Furthermore, different Ω will result in different effects, such as $\Omega = 0.1$ (anti-Unruh effect) and $\Omega = 2$ (Unruh effect) [19].

Recent studies have shown that the decoherence factor can also be used to distinguish the Unruh (anti-Unruh) phenomena [31]. Assume an Unruh–DeWitt detector coupled to the scalar field is in the following state initially

$$|\psi\rangle = (\alpha|g\rangle + \beta|e\rangle)|0\rangle . \tag{8}$$

After accelerating, the above state will evolve into

$$\begin{aligned} |\psi'\rangle &= \alpha C_+(|g\rangle|0\rangle - i\eta_+|e\rangle|1\rangle) + \beta C_-(|e\rangle|0\rangle + i\eta_-|g\rangle|1\rangle) \\ &= \alpha|g\rangle|\psi_0\rangle + \beta|e\rangle|\psi_1\rangle , \end{aligned} \tag{9}$$

where $|\psi_0\rangle = C_+|0\rangle + i(\beta/\alpha)C_-\eta_-|1\rangle$ and $|\psi_1\rangle = C_-|0\rangle - i(\alpha/\beta)C_+\eta_+|1\rangle$. The decoherence process can be quantified by the decoherence factor $D = |\langle\psi_0|\psi_1\rangle|$ [37]. The value of D ranges between 0 and 1, with larger values indicating stronger coherence. In general, the Unruh effect weakens coherence, while the anti-Unruh effect enhances it [31]. As shown in Fig. 2, coherence tends to increase with acceleration when $\Omega = 0.1$ and decrease with acceleration when $\Omega = 2$. Thus, we can infer that $\Omega = 0.1$ and 2 represent the anti-Unruh effect and the Unruh effect, respectively, under suitable conditions. This result is consistent with previous research that utilized transition probability to determine the occurrence of the Unruh effect or anti-Unruh effect [19].

3 The case of three detectors

In this study, we examine three identical Unruh–DeWitt detectors, A, B, and C, which are distant from each other and separately held by Alice, Bob, and Charlie. We assume the initial states of the detectors include two types of entangled states: the GHZ state and the W state, as follows:

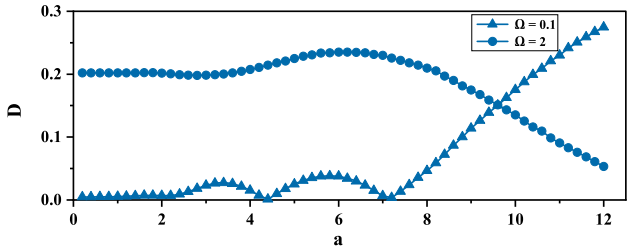

Fig. 2 The decoherence factor D as functions of the acceleration a with $\lambda = 0.1$, $\sigma = 0.4$, and $L = 200$. The various curves correspond to different values of Ω, specifically $\Omega = 0.1$ (blue triangles) and $\Omega = 2$ (blue circles)

$$\begin{aligned} |\psi\rangle_{ABC}^{GHZ} &= \frac{1}{\sqrt{2}}(|ggg\rangle + |eee\rangle)|000\rangle , \\ |\psi\rangle_{ABC}^{W} &= \frac{1}{\sqrt{3}}(|gge\rangle + |geg\rangle + |egg\rangle)|000\rangle , \end{aligned} \tag{10}$$

where we treat the vacuum as being in a product state. In subsequent sections, we will investigate three different scenarios in which one, two, or all three detectors are accelerating.

3.1 Alice in acceleration

Initially, we consider only Alice moving with constant acceleration. Applying the transformation from Eq. (6), the initial GHZ state transforms into the following form,

$$\begin{aligned} |\psi\rangle_{A'BC}^{GHZ} &= U_A|\psi\rangle_{ABC}^{GHZ} \\ &= \frac{1}{\sqrt{2}}(C_+|ggg000\rangle - iC_+\eta_+|egg100\rangle \\ &\quad + C_-|eee000\rangle + iC_-\eta_-|gee100\rangle). \end{aligned} \tag{11}$$

By tracing out the scalar field degrees of freedom, we can get the reduced density matrix $\rho_{A'BC}$ of three detectors,

$$\begin{pmatrix} \frac{1}{2}C_+^2 & 0 & 0 & 0 & 0 & 0 & 0 & \frac{1}{2}C_+C_-^* \\ 0 & 0 & 0 & 0 & 0 & 0 & 0 & 0 \\ 0 & 0 & 0 & 0 & 0 & 0 & 0 & 0 \\ 0 & 0 & 0 & \frac{1}{2}C_-^2\eta_-^2 & -\frac{1}{2}C_+^*C_-\eta_+^*\eta_- & 0 & 0 & 0 \\ 0 & 0 & 0 & -\frac{1}{2}C_+C_-^*\eta_+\eta_-^* & \frac{1}{2}C_+^2\eta_+^2 & 0 & 0 & 0 \\ 0 & 0 & 0 & 0 & 0 & 0 & 0 & 0 \\ 0 & 0 & 0 & 0 & 0 & 0 & 0 & 0 \\ \frac{1}{2}C_+^*C_- & 0 & 0 & 0 & 0 & 0 & 0 & \frac{1}{2}C_-^2 \end{pmatrix}.$$

where the density matrix is written in the basis $|ggg\rangle$, $|gge\rangle$, $|geg\rangle$, $|gee\rangle$, $|egg\rangle$, $|ege\rangle$, $|eeg\rangle$, $|eee\rangle$. Further, we can obtain the reduced density matrixes $\rho_{A'}$, ρ_B, ρ_C, $\rho_{A'B}$, $\rho_{A'C}$, and ρ_{BC}, and the TMI is given by

$$\begin{aligned} I_3 &= 2\cos^2\theta_+ \log(\cos\theta_+) + 2\sin^2\theta_+ \log(\sin\theta_+) \\ &\quad + 2\cos^2\theta_- \log(\cos\theta_-) + 2\sin^2\theta_- \log(\sin\theta_-) \\ &\quad - \frac{1}{2}(\sin^2\theta_+ + \sin^2\theta_-)\log(\sin^2\theta_+ + \sin^2\theta_-) \end{aligned}$$

$$-\frac{1}{2}(\cos^2\theta_+ + \sin^2\theta_-)\log(\cos^2\theta_+ + \sin^2\theta_-)$$
$$-\frac{1}{2}(\sin^2\theta_+ + \cos^2\theta_-)\log(\sin^2\theta_+ + \cos^2\theta_-)$$
$$-\frac{1}{2}(\cos^2\theta_+ + \cos^2\theta_-)\log(\cos^2\theta_+ + \cos^2\theta_-) + \log 2 \tag{12}$$

where $\cos\theta_\pm = C_\pm$ and $\sin\theta_\pm = C_\pm\eta_\pm$.

Similarly, the initial W state will become

$$\begin{aligned}|\psi\rangle^W_{A'BC} &= U_A|\psi\rangle^W_{ABC}\\ &= \frac{1}{\sqrt{3}}(C_+|gge000\rangle - iC_+\eta_+|ege100\rangle + C_+|geg000\rangle\\ &\quad - iC_+\eta_+|eeg100\rangle + C_-|egg000\rangle + iC_-\eta_-|ggg100\rangle).\end{aligned} \tag{13}$$

And we can also derive the reduced density matrix and the TMI.

Next, we plot the information delocalization quantified by TMI(I_3) as functions of acceleration a for both $\Omega = 2$ (Unruh effect) and $\Omega = 0.1$ (anti-Unruh effect) in Fig. 3. The lower two blue curves represent the initial GHZ state, while the upper two red curves correspond to the initial W state.

Noticeably, quantum information is delocalized in all four cases. When the initial state is GHZ state, the TMI value is approximately -1.0 for $\Omega = 0.1$, which is less than the value of around -0.8 for $\Omega = 2$. This relationship is also observed for the W state. When $\Omega = 0.1$, the TMI value is about -0.2, which is also smaller than the value of around -0.1 when $\Omega = 2$. The results suggest that the anti-Unruh effect leads to stronger delocalization of information. We believe that the main reason for this phenomenon is the different values of Ω. Specifically, the smaller the energy gap Ω, the greater the transition probability [19]. This implies that the maximally entangled state between detectors is more easily destroyed, resulting in information delocalization.

Moreover, the TMI value of the initial GHZ state is smaller than that of the initial W state. This demonstrates that detectors in the W initial state are more stable than those in the GHZ initial state under the influence of acceleration. This is consistent with our traditional understanding that the robustness of W state is stronger than that of GHZ state. For example, if the tripartite W state loses a qubit, the remaining two qubits are still entangled, while the tripartite GHZ state becomes a separable state.

3.2 Alice and Bob in acceleration

Then we let Alice and Bob move with the same acceleration while Charlie remains stationary. In this case, the initial states evolve into

$$|\psi\rangle^{GHZ}_{A'B'C} = U_AU_B|\psi\rangle^{GHZ}_{ABC}$$

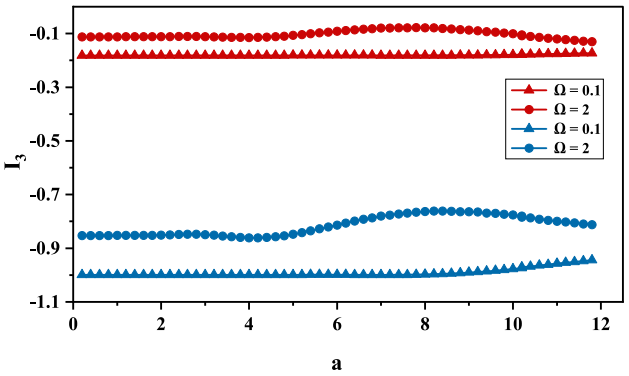

Fig. 3 The TMI as functions of the acceleration a when Alice is in acceleration. Here, blue curves and red curves represent that the initial state is GHZ state and W state respectively. The other parameters are the same as in Fig. 2

$$\begin{aligned}&= \frac{1}{\sqrt{2}}[C_+^2(|ggg000\rangle - i\eta_+|geg010\rangle - i\eta_+|egg100\rangle\\ &\quad - \eta_+^2|eeg110\rangle) + C_-^2(|eee000\rangle + i\eta_-|ege010\rangle\\ &\quad + i\eta_-|gee100\rangle - \eta_-^2|gge110\rangle)].\end{aligned} \tag{14}$$

and

$$\begin{aligned}|\psi\rangle^W_{A'B'C} &= U_AU_B|\psi\rangle^W_{ABC}\\ &= \frac{1}{\sqrt{3}}[C_+^2(|gge000\rangle - i\eta_+|gee010\rangle - i\eta_+|ege100\rangle\\ &\quad - \eta_+^2|eee110\rangle) + C_+C_-(|geg000\rangle + i\eta_-|ggg010\rangle\\ &\quad - i\eta_+|eeg100\rangle + \eta_+\eta_-|egg110\rangle + |egg000\rangle\\ &\quad - i\eta_+|eeg010\rangle + i\eta_-|ggg100\rangle + \eta_+\eta_-|geg110\rangle)].\end{aligned} \tag{15}$$

Adopting the approach used in the previous case, we obtain the expression for TMI and plot TMI (I_3) as functions of acceleration a (refer to Fig. 4). Notably, there are similarities between Figs. 4 and 3. In the case of the initial GHZ state, the TMI value is about -1.0 at $\Omega = 0.1$, which is lower than the TMI value of about -0.7 at $\Omega = 2$. The same rules can be observed in the initial W state. Besides, the TMI value of the initial GHZ state is smaller than the value of the initial W state, which is the same phenomenon as observed in Fig. 3. As a result, we can draw a parallel conclusion to that of Fig. 3, namely, the anti-Unruh effect leads to greater information delocalization, and the W state exhibits greater robustness compared to the GHZ state under identical conditions.

3.3 All in acceleration

Next, we examine the third situation that Alice, Bob, and Charlie all move with constant acceleration. By the transfor-

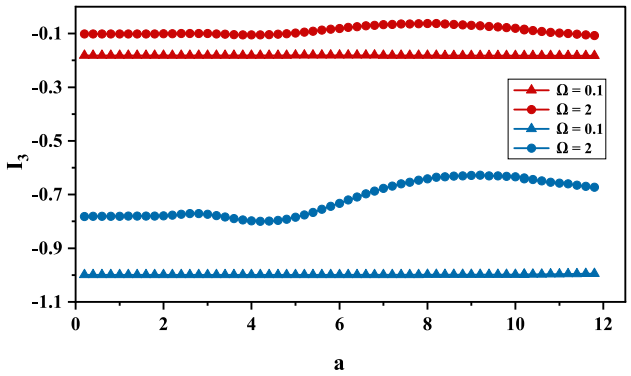

Fig. 4 The TMI as functions of the acceleration a when Alice and Bob are in acceleration. Here, blue curves and red curves represent that the initial state is GHZ state and W state respectively. The other parameters are the same as in Fig. 2

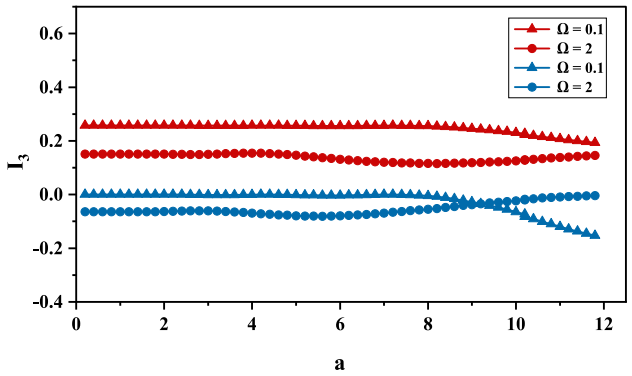

Fig. 5 The TMI as functions of the acceleration a when All are in acceleration. Here, blue curves and red curves represent that the initial state is GHZ state and W state respectively. The other parameters are the same as in Fig. 2

mation of Eq. (6), we can obtain

$$\begin{aligned}|\psi\rangle^{GHZ}_{A'B'C'} &= U_A U_B U_C |\psi\rangle^{GHZ}_{ABC} \\ &= \frac{1}{\sqrt{2}}[C_+^3(|ggg000\rangle - i\eta_+ |gge001\rangle - i\eta_+ |geg010\rangle \\ &\quad - \eta_+^2 |gee011\rangle - i\eta_+ |egg100\rangle - \eta_+^2 |ege101\rangle \\ &\quad - \eta_+^2 |eeg110\rangle + i\eta_+^3 |eee111\rangle) + C_-^3(|eee000\rangle \\ &\quad + i\eta_- |eeg001\rangle + i\eta_- |ege010\rangle - \eta_-^2 |egg011\rangle \\ &\quad + i\eta_- |gee100\rangle - \eta_-^2 |geg101\rangle - \eta_-^2 |gge110\rangle \\ &\quad - i\eta_-^3 |ggg111\rangle)], \end{aligned} \tag{16}$$

and

$$\begin{aligned}|\psi\rangle^{W}_{A'B'C'} &= U_A U_B U_C |\psi\rangle^{W}_{ABC} \\ &= \frac{1}{\sqrt{3}} C_+^2 C_-(|gge000\rangle + i\eta_- |ggg001\rangle - i\eta_+ |gee010\rangle \\ &\quad + \eta_+\eta_- |geg011\rangle - i\eta_+ |ege100\rangle + \eta_+\eta_- |egg101\rangle \\ &\quad - \eta_+^2 |eee110\rangle - i\eta_+^2\eta_- |eeg111\rangle + |geg000\rangle \\ &\quad - i\eta_+ |gee001\rangle + i\eta_- |ggg010\rangle + \eta_+\eta_- |gge011\rangle \\ &\quad - i\eta_+ |eeg100\rangle - \eta_+^2 |eee101\rangle + \eta_+\eta_- |egg110\rangle \\ &\quad - i\eta_+^2\eta_- |ege111\rangle + |egg000\rangle - i\eta_+ |ege001\rangle \\ &\quad - i\eta_+ |eeg010\rangle - \eta_+^2 |eee011\rangle + i\eta_- |ggg100\rangle \\ &\quad + \eta_+\eta_- |gge101\rangle + \eta_+\eta_- |geg110\rangle - i\eta_+^2\eta_- |gee111\rangle). \end{aligned} \tag{17}$$

Similarly, we can plot TMI (I_3) as functions of acceleration a (refer to Fig. 5). It is noteworthy that the sign of TMI is positive for the case of initial W state, where the TMI value is about 0.25 for $\Omega = 0.1$ and 0.15 for $\Omega = 2$. Based on previous analyses, this suggests that quantum information is not distributed to the entire system when three Unruh–DeWitt detectors in the W state undergo identical acceleration. Moreover, compared with Figs. 3 and 4, we note that the TMI values in Fig. 5 are larger under the same conditions. This contrasts with the anticipated outcome that as more detectors accelerate, more information should be delocalized. However, our observations suggest that information delocalization is weaker when all three detectors are accelerating compared to when one or two detectors are accelerating. The information, in fact, is not only delocalized but also transferred into the vacuum when the detectors are accelerated. Therefore, as the number of acceleration detectors increases, more information may leak into the vacuum rather than being dispersed throughout the entire system, resulting in the weakening of information delocalization.

Additionally, we notice that the TMI value of the initial GHZ state is essentially 0 for $\Omega = 0.1$ when the acceleration is relatively small ($a \leq 8$), indicating that information delocalization does not occur. However, as the acceleration continues to increase, the TMI value for $\Omega = 0.1$ decreases rapidly and becomes smaller than the TMI value for $\Omega = 2$. That is, compared with the Unruh effect, the anti-Unruh effect does not cause information delocalization at the beginning of acceleration, but it quickly leads to stronger information delocalization as acceleration increases. We also observe that the TMI value of the initial GHZ state is lower than the TMI value of the initial W state. This relationship is the same as in the previous two situations. Although different from Figs. 3 and 4, we can still reach the same conclusion that the anti-Unruh effect contributes to stronger information delocalization throughout the system, and the initial W state results in weaker or even nonexistent information delocalization.

4 The case of multiple detectors

For the N detectors case, the calculation of TMI is much more complicated. Here, we only discuss the N-partite GHZ state and N-partite product state.

4.1 N-partite GHZ state

Consider the N-partite GHZ state,

$$|\psi\rangle^{GHZ}_{1,2,\ldots,N} = \frac{1}{\sqrt{2}}(|gg\ldots g\rangle + |ee\ldots e\rangle)\,|00\ldots 0\rangle\,. \quad (18)$$

Assume the number of detectors in acceleration is L,

$$\begin{aligned}|\psi\rangle^{GHZ}_{1',2',\ldots,L',\ldots,N} &= U_1U_2\ldots U_L\,|\psi\rangle^{GHZ}_{1,2,\ldots,N}\\ &= C_+^L(|g\rangle|0\rangle - i\eta_+|e\rangle\,|1\rangle_m)^{\otimes L}\otimes|g0\rangle\otimes\cdots\otimes|g0\rangle\\ &\quad + C_-^L(|e\rangle|0\rangle + i\eta_-|g\rangle\,|1\rangle_m)^{\otimes L}\otimes|e0\rangle\otimes\cdots\otimes|e0\rangle\,. \quad (19)\end{aligned}$$

Now, we can employ two distinct methods to partition the N-partite system into three subsystems: A, B, and C. In the first method, all detectors in acceleration are designated as subsystem A, and the remaining detectors are divided equally between subsystems B and C. The second method involves equally assigning the detectors in acceleration to subsystems A and B, and allocating the remaining detectors to subsystem C. In the first method, we can calculate the TMI and obtain the TMI(I_3) as functions of the acceleration a for $L = 1, 2, 3$, or 4, as depicted in Fig. 6. Notably, the TMI value at $\Omega = 0.1$ is less than that at $\Omega = 2$, that is to say, the anti-Unruh effect results in stronger information delocalization. We also find that the TMI value increases as the number of detectors in acceleration increases. Although this phenomenon is not apparent when $\Omega = 0.1$, it becomes evident as the acceleration increases ($a \geq 8.5$). Hence, our previous explanation of why the TMI value for all three detectors in acceleration is larger than the TMI value for one or two detectors in acceleration is reasonable. This suggests that information delocalization indeed diminishes as the number of detectors in acceleration increases.

In the second method, we can also derive the TMI expression and obtain the TMI(I_3) as functions of the acceleration a when $L = 2$ or 4, as illustrated in Fig. 7. We can easily observe similar phenomena to Fig. 6. Consequently, we can once again conclude, in line with the previous sections, that the anti-Unruh effect induces greater delocalization of information and more detectors in acceleration can attenuate information delocalization.

4.2 N-partite product state

In the preceding section, we presented the evolution of TMI when the detectors are in entangled states. Nevertheless, there may initially be no correlation between the three detectors. Assume the initial state of detectors is a product state, such as $|\psi\rangle_{1,2,\ldots,N} = |eg\ldots g\rangle\,|00\ldots 0\rangle$. If the first detector is in acceleration, we can easily derive that $\rho_{1',2,\ldots,N} = \rho_{1'}\otimes\rho_2\otimes\cdots\otimes\rho_N$. This shows that the new reduced density matrix is still separable and the TMI remains

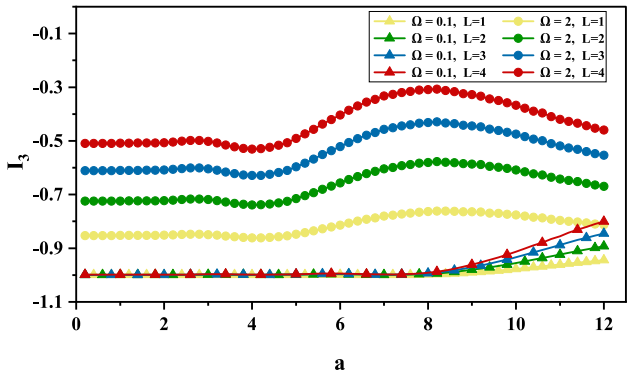

Fig. 6 The TMI as functions of the acceleration a in N detectors case for the first method when $L = 1$, 2, 3, or 4. The other parameters are the same as in Fig. 2

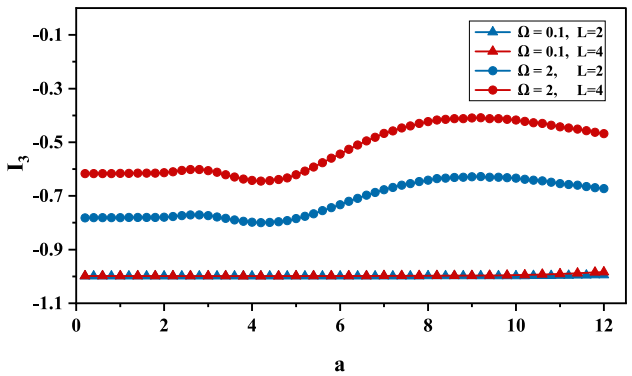

Fig. 7 The TMI as functions of the acceleration a in N detectors case for the second method when $L = 2$ or 4. The other parameters are the same as in Fig. 2

zero. By simply recalculating, we can also obtain a similar result when two or more detectors are in acceleration. In fact, this phenomenon is not difficult to understand. There is no channel to propagate information because only the first-order approximation is considered and the evolution of each detector is independent of each other. Naturally, the uncorrelated Unruh–DeWitt detectors remain separate. In other words, it is impossible to create entanglement through accelerating separable detectors [31]. The above observations demonstrate that information delocalization does not occur when the detectors are initially in a product state.

5 Conclusions

In summary, we employed the Unruh–DeWitt model to systematically investigate the impact of acceleration on information delocalization in cases involving the Unruh effect and the anti-Unruh effect. Our numerical calculations reveal that more quantum information is delocalized under the anti-Unruh effect because the corresponding energy gap is smaller. We also observed that the information delocaliza-

tion may diminish as more and more Unruh–DeWitt detectors are accelerated since information can also be transferred into the vacuum. In addition, we found that the GHZ state is more susceptible to acceleration and generates greater information delocalization than the W state. We also extended our analysis to the N-detector case, i.e., the N-partite GHZ state, and found results consistent with the tripartite system. Finally, we demonstrated that information is not delocalized when the detectors are initially in a product state. Recent studies have identified a phenomenon similar to the anti-Unruh effect in certain physical situations, known as the anti-Hawking effect [38,39]. Further exploration using the methods presented in this paper can also contribute to our understanding of the Hawking effect and the anti-Hawking effect.

Acknowledgements The author thanks Qing-yu Cai and Baocheng Zhang for valuable discussions and comments. This work was supported by the National Natural Science Foundation of China under Grant No. 11725524.

Data Availability Statement This manuscript has no associated data or the data will not be deposited. [Authors' comment: This is a theoretical study without any experimental data.]

Funded by SCOAP^3. SCOAP^3 supports the goals of the International Year of Basic Sciences for Sustainable Development.

References

1. E. Altman, Many-body localization and quantum thermalization. Nat. Phys. **14**, 979 (2018)
2. E. Iyoda, T. Sagawa, Scrambling of quantum information in quantum many-body systems. Phys. Rev. A **97**, 042330 (2018)
3. S. Sahu, S. Xu, B. Swingle, Scrambling dynamics across a thermalization-localization quantum phase transition. Phys. Rev. Lett. **123**, 165902 (2019)
4. K. Yamaguchi, N. Watamura, M. Hotta, Quantum information capsule and information delocalization by entanglement in multiple-qubit systems. Phys. Lett. A **383**, 1255–1259 (2019)
5. D. Wanisch, S. Fritzsche, Delocalization of quantum information in long-range interacting systems. Phys. Rev. A **104**, 042409 (2021)
6. A. Soeda, M. Murao, Delocalization power of global unitary operations on quantum information. New J. Phys. **12**, 093013 (2010)
7. J. Miguel-Ramiro, W. Dür, Delocalized information in quantum networks. New J. Phys. **22**, 043011 (2020)
8. P. Hayden, J. Preskill, Black holes as mirrors: quantum information in random subsystems. J. High Energy Phys. **2007**, 120 (2007)
9. A. Bhattacharyya, L.K. Joshi, B. Sundar, Quantum information scrambling: from holography to quantum simulators. Eur. Phys. J. C **82**, 458 (2022)
10. P. Hosur, X.-L. Qi, D.A. Roberts, B. Yoshida, Chaos in quantum channels. J. High Energy Phys. **2016**, 4 (2016)
11. C. Sünderhauf, L. Piroli, X.-L. Qi, N. Schuch, J.I. Cirac, Quantum chaos in the Brownian SYK model with large finite N: OTOCs and tripartite information. J. High Energy Phys. **2019**, 38 (2019)
12. W.G. Unruh, Notes on black-hole evaporation. Phys. Rev. D **14**, 870 (1976)
13. S.W. Hawking, Black hole explosions? Nature **248**, 30 (1974)
14. S.W. Hawking, Particle creation by black holes. Commun. Math. Phys. **43**, 199 (1975)
15. G.W. Gibbons, S.W. Hawking, Cosmological event horizons, thermodynamics, and particle creation. Phys. Rev. D **15**, 2738 (1977)
16. T. Jacobson, Thermodynamics of spacetime: the Einstein equation of state. Phys. Rev. Lett. **75**, 1260 (1995)
17. E. Verlinde, On the origin of gravity and the laws of Newton. J. High Energy Phys. **2011**, 29 (2011)
18. B.S. DeWitt, Quantum gravity: the new synthesis, in *General Relativity: An Einstein Centenary Survey*, ed. by S.W. Hawking, W. Israel (Cambridge University Press, Cambridge, 1979), p. 680
19. W.G. Brenna, R.B. Mann, E. Martín-Martínez, Anti-Unruh phenomena. Phys. Lett. B **757**, 307 (2016)
20. L.J. Garay, E. Martín-Martínez, J. de Ramón, Thermalization of particle detectors: the Unruh effect and its reverse. Phys. Rev. D **94**, 104048 (2016)
21. I. Fuentes-Schuller, R.B. Mann, Alice falls into a black hole: entanglement in noninertial frames. Phys. Rev. Lett. **95**, 120404 (2005)
22. P.M. Alsing, I. Fuentes-Schuller, R.B. Mann, T.E. Tessier, Entanglement of Dirac fields in noninertial frames. Phys. Rev. A **74**, 032326 (2006)
23. D.E. Bruschi, J. Louko, E. Martín-Martínez, A. Dragan, I. Fuentes, Unruh effect in quantum information beyond the single-mode approximation. Phys. Rev. A **82**, 042332 (2010)
24. E. Martín-Martínez, J. León, Fermionic entanglement that survives a black hole. Phys. Rev. A **80**, 042318 (2009)
25. E. Martín-Martínez, L.J. Garay, J. León, Unveiling quantum entanglement degradation near a Schwarzschild black hole. Phys. Rev. D **82**, 064006 (2010)
26. J. Wang, J. Jing, Multipartite entanglement of fermionic systems in noninertial frames. Phys. Rev. A **83**, 022314 (2011)
27. D.E. Bruschi, A. Dragan, I. Fuentes, J. Louko, Particle and antiparticle bosonic entanglement in noninertial frames. Phys. Rev. D **86**, 025026 (2012)
28. M. Shamirzaie, B.N. Esfahani, M. Soltani, Tripartite entanglements in noninertial frames. Int. J. Theor. Phys. **51**, 787 (2012)
29. B. Richter, Y. Omar, Degradation of entanglement between two accelerated parties: Bell states under the Unruh effect. Phys. Rev. A **92**, 022334 (2015)
30. Y. Dai, Z. Shen, Y. Shi, Killing quantum entanglement by acceleration or a black hole. J. High Energy Phys. **2015**, 71 (2015)
31. T. Li, B. Zhang, L. You, Would quantum entanglement be increased by anti-Unruh effect? Phys. Rev. D **97**, 045005 (2018)
32. Y. Pan, B. Zhang, Influence of acceleration on multibody entangled quantum states. Phys. Rev. A **101**, 062111 (2020)
33. Y. Pan, B. Zhang, Anti-Unruh effect in the thermal background. Phys. Rev. D **104**, 125014 (2021)
34. S.-M. Wu, H.-S. Zeng, T. Liu, Genuine multipartite entanglement subject to the Unruh and anti-Unruh effects. New J. Phys. **24**, 073004 (2022)
35. P.M. Alsing, G.J. Milburn, Teleportation with a uniformly accelerated partner. Phys. Rev. Lett. **91**, 180404 (2003)
36. P.M. Alsing, D. McMahon, G.J. Milburn, Teleportation in a noninertial frame. J. Opt. B: Quantum Semiclass. Opt. **6**, S834 (2004)

37. A. Bassi, K. Lochan, S. Satin, T.P. Singh, H. Ulbricht, Models of wave-function collapse, underlying theories, and experimental tests. Rev. Mod. Phys. **85**, 471 (2013)
38. L.J. Henderson, R.A. Hennigar, R.B. Mann, A.R. Smith, J. Zhang, Anti-Hawking phenomena. Phys. Lett. B **809**, 135732 (2020)
39. M.P. Robbins, R.B. Mann, Anti-Hawking phenomena around a rotating BTZ black hole. Phys. Rev. D **106**, 045018 (2022)